GeoHealth

RESEARCH ARTICLE
10.1029/2021GH000390

Key Points:

- A multi-model ensemble of CMIP6 models performs well in simulating temporal changes of warm/wet extremes
- The inter-model uncertainties for the frequencies of compound warm extremes are considerably higher than those of compound cold extremes
- The projected uncertainties in the global occurrences of warm/wet extremes are 3.82 times those of warm/dry extremes during 2070–2099

Supporting Information:

Supporting Information may be found in the online version of this article.

Correspondence to:

C. Miao,
miaocy@vip.sina.com

Citation:

Wu, Y., Miao, C., Sun, Y., AghaKouchak, A., Shen, C., & Fan, X. (2021). Global observations and CMIP6 simulations of compound extremes of monthly temperature and precipitation. *GeoHealth*, *5*, e2021GH000390. https://doi.org/10.1029/2021GH000390

Received 17 JAN 2021
Accepted 17 APR 2021

Author Contributions:

Conceptualization: Ying Sun, Amir AghaKouchak
Data curation: Chiyuan Miao, Ying Sun, Chenwei Shen, Xuewei Fan
Formal analysis: Yi Wu
Funding acquisition: Chiyuan Miao
Methodology: Chiyuan Miao, Ying Sun, Amir AghaKouchak, Xuewei Fan
Software: Chenwei Shen
Supervision: Chiyuan Miao

Global Observations and CMIP6 Simulations of Compound Extremes of Monthly Temperature and Precipitation

Yi Wu[1], Chiyuan Miao[1], Ying Sun[2], Amir AghaKouchak[3], Chenwei Shen[1], and Xuewei Fan[1]

[1]State Key Laboratory of Earth Surface Processes and Resource Ecology, Faculty of Geographical Science, Beijing Normal University, Beijing, China, [2]National Climate Center, Laboratory for Climate Studies, China Meteorological Administration, Beijing, China, [3]Center for Hydrometeorology and Remote Sensing, Department of Civil and Environmental Engineering, University of California, Irvine, CA, USA

Abstract Compound climate extremes, such as events with concurrent temperature and precipitation extremes, have significant impacts on the health of humans and ecosystems. This paper aims to analyze temporal and spatial characteristics of compound extremes of monthly temperature and precipitation, evaluate the performance of the sixth phase of the Coupled Model Intercomparison Project (CMIP6) models in simulating compound extremes, and investigate their future changes under Shared Socioeconomic Pathways (SSPs). The results show a significant increase in the frequency of compound warm extremes (warm/dry and warm/wet) but a decrease in compound cold extremes (cold/dry and cold/wet) during 1985–2014 relative to 1955–1984. The observed upward trends of compound warm extremes over China are much higher than those worldwide during the period of interest. A multi-model ensemble (MME) of CMIP6 models performs well in simulating temporal changes of warm/wet extremes, and temporal correlation coefficients between MME and observations are above 0.86. Under future scenarios, CMIP6 simulations show substantial rises in compound warm extremes and declines in compound cold extremes. Globally, the average frequency of warm/wet extremes over a 30-yr period is projected to increase for 2070–2099 relative to 1985–2014 by 18.53, 34.15, 48.79, and 59.60 under SSP1-2.6, SSP2-4.5, SSP3-7.0, and SSP5-8.5, respectively. Inter-model uncertainties for the frequencies of compound warm extremes are considerably higher than those of compound cold extremes. The projected uncertainties in the global occurrences of warm/wet extremes are 3.82 times those of warm/dry extremes during 2070–2099 and especially high for the Amazon and the Tibetan Plateau.

Plain Language Summary Compound climate extremes, such as the events with concurrent temperature and precipitation extremes, have significant impacts on the health of humans and ecosystems. Can climate model simulate the historical compound extremes? If yes, how the global compound extremes will change in the future? In this study, we found that the global climate model performs well in simulating temporal changes of warm/wet and warm/dry extremes during the period 1955–2014. With greenhouse gas emissions continuing to increase in the future, compound warm/dry and warm/wet extremes show a continuous increase in frequency in the next few decades, while compound cold/dry and cold/wet extremes are projected to occur less frequently.

1. Introduction

Future climate change will not only affect mean climate but will also likely alter the frequency and magnitude of extreme climate events (Fischer & Knutti, 2015; Miao et al., 2014; Wu et al., 2020). Here, we broadly define an "extreme" event as a rare and infrequent occurrence at a specific time and site. It is a low-probability event corresponding to a certain climate variable from either of the tails of that variable's probability density function (Seneviratne et al., 2012). Specifically, we usually define extreme events as those that occur in the highest or lowest 5% (Casanueva et al., 2013; Vincent et al., 2018) or 10% (Beniston & Stephenson, 2004; Seneviratne et al., 2012) of historical measurements, or two standard deviations from the mean (Ding et al., 2019; Rahmstorf & Coumou, 2011). Numerous studies have shown that the frequency of extreme events has increased regionally and globally (Seneviratne et al., 2012; Sun et al., 2014). In

Validation: Yi Wu, Xuewei Fan
Visualization: Yi Wu
Writing – original draft: Yi Wu, Chiyuan Miao
Writing – review & editing: Chiyuan Miao, Ying Sun, Amir AghaKouchak

the context of climate change (Gou et al., 2021), the consequences of climate extremes for human health (Sun et al., 2019; Yang et al., 2019), food security (Eggen et al., 2019), and other socioeconomic factors have been widely recognized worldwide. There is an extensive body of literature on univariate extreme events based on observations over the past several decades, and these studies commonly rely on analyzing extreme climate indices derived for one variable at a time (e.g., precipitation, temperature) (Papalexiou & Montanari, 2019; Wang et al., 2019).

However, most climate extreme events are essentially interrelated, and a multivariate approach might be necessary to capture how different extreme events interact with each other. Temperature and precipitation are two key climatic variables that may respond to various but related internal and external climate forcings on both shorter and longer time scales (Liu et al., 2018). The concurrence of multiple hazards or events leading to significant impacts on ecosystem and society across multiple temporal and spatial scales is termed a "compound event" (Zscheischler & Seneviratne, 2017), although the individual drivers/hazards involved may not be severe (Leonard et al., 2014). Meanwhile, concurrences of multiple types of extremes (e.g., droughts and heat waves) typically have broader and more significant impacts on natural and social environments compared with individual occurrences (Zscheischler & Seneviratne, 2017). For instance, heat waves are often accompanied by below-average precipitation, such as in the 2003 European (Fink et al., 2004) and 2010 Russian (Trenberth & Fasullo, 2012) heat waves, both of which caused devastating economic losses. Furthermore, analysis of individual extreme events may lead to underestimation of the effects of interrelated extremes and compound events (Leonard et al., 2014; Sadegh et al., 2018). Detection and quantification of changes in the concurrence of extremes in temperature and precipitation under a warming climate are important for making reliable risk projections and for understanding changes in characteristics of compound extremes and their associated uncertainties, which will provide helpful information for policy making and project planning (Seneviratne et al., 2012). Among the various types of compound extremes, concurrent droughts and heat waves have received a great deal of attention in recent years, and based on observations, compound extremes (especially warm/dry conditions) increased significantly in the second half of the 20th century (Li et al., 2019; Miao et al., 2016; Sharma & Mujumdar, 2017).

Due to the uncertainties of the climate system itself (Zhou & Chen, 2015) and interactions among climate variables, it is extremely difficult to accurately simulate and predict changes in compound climate extremes in the past and future. Global climate models (GCMs) have been widely used to study extreme weather and climate events, and these models can reproduce climate extremes to some extent (You et al., 2018). The most recent suite of climate models was developed to participate in the sixth phase of the Coupled Model Intercomparison Project (CMIP6). Compared with the previous phases of the CMIP, CMIP6 fills some of the main scientific gaps, such as the identification of systematic model errors and the simulation and estimation of radiative forcing in the past and future (Eyring et al., 2019). With respect to the scenarios used to guide projections of the future, a set of Shared Socioeconomic Pathways (SSPs) has been proposed as the latest generation of scenarios for long-term experiments (Riahi et al., 2017). Recent research has shown that CMIP6 has made some progress in simulating temperature (Nie et al., 2020) and precipitation (Gusain et al., 2020; Tian & Dong, 2020) compared with CMIP5.

Assessment of compound extremes using climate models is important both for researchers from various fields who will use the model output and for modelers working on further model development. In order to evaluate the performance of CMIP5 historical simulation for compound extremes, Hao et al. (2013) assessed the occurrence of concurrent monthly precipitation and temperature extremes for warm/wet, warm/dry, cold/wet, and cold/dry concurrences from 1951 to 2004 over global land. Zscheischler and Seneviratne (2017) analyzed the global concurrence of hot and dry summers from 1901 to 2013, they showed that the impacts of compound extremes were more serious than the impacts of independent hot or dry extremes. Also, Hao et al. (2019) used observations and simulations to assess climate change impacts on the dependence between precipitation and temperature during the period 1951–2004 over global land areas. For the future scenarios, Estrella and Menzel (2013) investigated recent and future climate extremes arising from changes to the bivariate distribution of temperature and precipitation in Bavaria, Germany; and Zhou and Liu (2018) analyzed the likelihood of concurrent climate extremes and variations over China. However, quantitative studies of the performance of model simulations in reproducing compound extremes are relatively rare, and current research has mainly focused on historical variation in compound extremes;

furthermore, investigations into future compound extremes have seldom addressed global scales. Additionally, to the best of our knowledge, changes in statistics of future compound extremes have not been investigated using CMIP6 simulations. A comprehensive analysis of changes in compound extremes using CMIP6 will help in (a) understanding the strength and limitations of current CMIP6 models in reproducing historical compound extremes and (b) updating our projections of changes in concurrent extremes under new scenarios of the future. Therefore, this paper aims to analyze the temporal and spatial characteristics of compound extremes of monthly temperature and precipitation, to evaluate the performance of 16 CMIP6 models in simulating compound extremes, and to investigate future changes and uncertainties of compound extremes under four SSP scenarios.

2. Data and Methods

2.1. Data

2.1.1. Observational Data

To better evaluate the performance of the different CMIP6 models, we used two observational data sets in our study. For the first, we obtained global observation data of monthly mean surface air temperature and monthly total precipitation spanning 1901–2018 from the gridded Climatic Research Unit (CRU) Time-series product (version 4.03) (Harris et al., 2014) (https://crudata.uea.ac.uk/cru/data/hrg/cru_ts_4.03/). For the second, we selected the land surface air temperature data set from the Global Historical Climatology Network version 2 and the Climate Anomaly Monitoring System (GHCN + CAMS) (Fan & van den Dool, 2008) (https://www.psl.noaa.gov/data/gridded/data.ghcncams.html) and NOAA's Precipitation Reconstruction over Land (PREC/L) data set (Chen et al., 2002) (http://www.psl.noaa.gov/data/gridded/data.precl.html), spanning 1948–2020, along with their station observations collected from GHCN + CAMS. We will refer to this data set as GHCN_CAMS in later text. These two data sets are available across global land areas at a high grid resolution of $0.5° \times 0.5°$. However, only the land area north of 60°S is considered for the observations and model outputs in this study because the CRU data set does not provide data for Antarctica.

2.1.2. Model Data

Model output data of monthly mean surface air temperature and monthly total precipitation are from 16 CMIP6 GCMs (Table S1; data available at https://esgf-node.llnl.gov/projects/cmip6/). Historical simulations (1955–2014) and future projections (2040–2099) under four SSPs are involved in this study. The SSPs address both socioeconomic and technological development and are used to fill gaps in previous Representative Concentration Pathways (RCPs) studies in CMIP5 (O'Neill et al., 2016). Tier-1 scenarios that span a wide range of uncertainties in future forcing are considered in our study (including SSP1-2.6, SSP2-4.5, SSP3-7.0, and SSP5-8.5, in order of increasing forcing level), which is designed to provide a full range of forcing targets similar in both magnitude and distribution to the RCPs used in CMIP5 (Gidden et al., 2019) (Table S2).

2.2. Methodology

As in previous studies (Diaconescu et al., 2015; Kim et al., 2020; Semmler et al., 2020), prior to the analysis, the observational data and all CMIP6 output were re-gridded to the same spatial resolution ($1° \times 1°$), using bilinear interpolation. Only one realization from each model is used here so that the performance of each model can be compared on an equal basis. Multi-model ensembles (MMEs) were constructed by applying equal weights to all 16 models in this study.

The thresholds for compound extremes of temperature and precipitation in this paper are defined by selecting 10% and 90% quantiles following the example of the Intergovernmental Panel on Climate Change (IPCC) (Seneviratne et al., 2012). The thresholds are calculated by using the monthly temperature and precipitation for each month of the 30-yr period 1955–1984. The occurrence of compound temperature and precipitation extremes here represents when two extreme events occur in the same month. Four types of modes of compound extremes are defined for detailed analysis: warm/dry ($T90/P10$), warm/wet ($T90/P90$), cold/dry ($T10/P10$), and cold/wet ($T10/P90$), where T stands for temperature and P stands for precipitation. In other words, compound extremes are defined as months when abnormal conditions occur for

both temperature and precipitation that are above or below the thresholds that have been defined from the period 1955–1984. $T10$ and $P10$ indicate that the occurrence frequencies of temperature and precipitation, respectively, are below the 10% quantile, while $T90$ and $P90$ denote that the occurrence frequencies are above the 90% quantile.

For investigating the regional-scale performance of the models in the future, the global land area (excluding Antarctica) is divided into 26 subregions based on the definitions of the IPCC Special Report on Managing the Risks of Extreme Events and Disasters to Advance Climate Change Adaptation (Seneviratne et al., 2012), and exact coordinates of the regions are provided in Table S3. This set of region definitions has been widely adopted in previous studies (Ciavarella et al., 2017).

We compared percentage changes (PCs) in the number of compound climate extremes during the period 1955–1984. We focused this research on the period 1955–2014 for three main reasons: First, the historical simulation data of the CMIP6 models extends to 2014. Second, we need observational data to be able to evaluate the model performance. Meteorological observation sites were relatively sparse before the middle of the 20th century, and data quality in earlier years is less reliable, so we chose the 1950s as the starting point for our research. Third, to define two 30-yr average time series that we could fairly compare, we selected 1955–1984 as the first period and 1985–2014 as the second period. The number of compound extreme events of each period is calculated by counting the frequency of compound events of $T90/P10$, $T90/P90$, $T10/P10$, and $T10/P90$ at each grid point. The PC is estimated as follows:

$$\mathrm{PC} = 100 \times \frac{P_2 - P_1}{P_1} \tag{1}$$

where P_1 is the number of compound extreme events in the first period (1955–1984) and P_2 is the number of compound extreme events in the second period (1985–2014).

Probability of detection (POD) (Dinku et al., 2010) analysis is conducted to describe the capability of detecting change (increase, decrease, or neutral) in the number of compound extremes identified in the CMIP6 model output with respect to CRU and GHCN_CAMS observations. The concept of POD is used in various industries to establish the ability to detect defects, and it relates the POD to the characteristic parameter of the defect. Here, POD describes what fraction of the observed compound extreme events is detected by the model output. The formula is as follows:

$$\mathrm{POD} = \frac{N_1}{N_2} \tag{2}$$

where N_1 is the number of grid cells in the simulation or ensemble that show the same direction of change (increase, decrease, or neutral) as the observation, while N_2 is the total number of land grid cells (excluding Antarctica).

Finally, we calculate the changes in the absolute numbers of compound extremes grid cell by grid cell by comparing the model output for two future periods, 2040–2069 (medium term) and 2070–2099 (long term), relative to the period 1985–2014. We analyze the inter-model uncertainties of change in the number of compound extremes under the four SSPs by using box plots that illustrate a collection of descriptive statistics to highlight salient features of the data.

3. Results and Discussion

3.1. Percentage Changes in Number of Compound Extremes

The warm/dry extreme, which usually corresponds to concurrence of heat waves and droughts, is the most studied and the most influential type of event among the four types of compound extremes considered in this paper (Li et al., 2019; Sharma & Mujumdar, 2017; Zscheischler & Seneviratne, 2017). According to the CRU and GHCN_CAMS observations, warm/dry extremes have increased in many regions worldwide, including notable increases in Africa, East Asia (especially China), and eastern Australia, and also slight increases in some areas such as the Amazon and Greenland (Figure 1). Percentage increases in the number

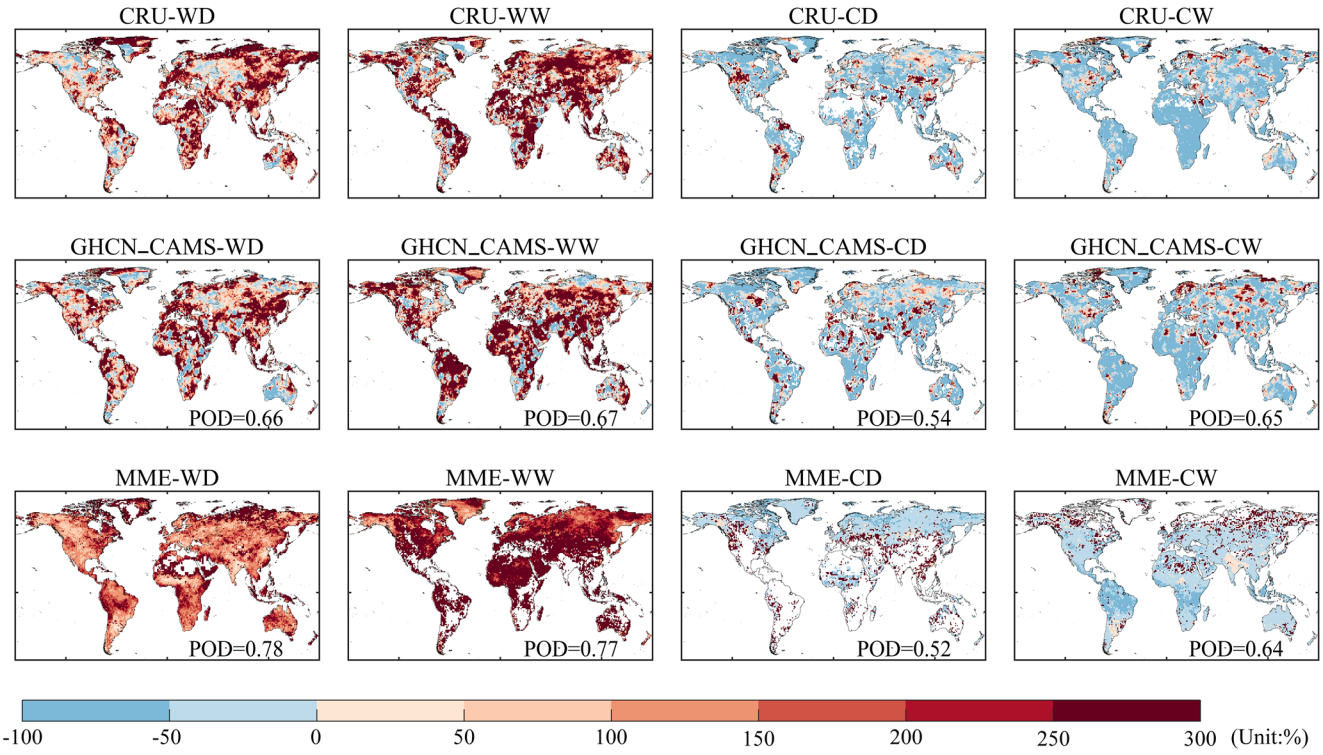

Figure 1. Percentage changes in the occurrences of the warm/dry (WD), warm/wet (WW), cold/dry (CD), and cold/wet (CW) extremes for the period 1985–2014 relative to 1955–1984 in the observations and the MME. The values in the lower right corner are the POD values with CRU as the reference.

of warm/dry extremes in most parts of the world exceed 100%. Existing research also showed that significant increases in the severity of compound dry and hot events occurred in most parts of China during the past few decades (Wu et al., 2020). CRU and GHCN_CAMS observation data reveal an overall increase in the number of warm/wet extremes globally during the period 1985–2014 relative to 1955–1984 (i.e., concurrence of high temperatures and heavy precipitation), and the PCs exceed 200% over most regions. Similar findings have appeared in previous studies (Wasko & Sharma, 2017; Zhang & Villarini, 2017), which also revealed a continuous increase in warm/wet compound events. Similar to the warm/dry extremes, the warm/wet extremes also appear to increase in tropical and high-latitude regions (Figure S1). Globally, Africa, the eastern part of South America, the Middle East, East Asia (especially China), and South Asia have larger increases in occurrences of warm/wet extremes than other regions worldwide. A recent study found that there have been increasing occurrences of extremely humid and hot weather that had been rare or unprecedented in the past in Asia, Africa, Australia, South America, and North America (including the US Gulf Coast) (Raymond et al., 2020). Many studies have shown that extreme temperature and precipitation events increased in the second half of the 20th century (Donat et al., 2016; Oliver et al., 2018; Zhou et al., 2016). This indicates, to some extent, that temperature- and precipitation-related extreme events (both independent and compound) have shown an increasing trend over the past few decades. By contrast, according to the CRU and GHCN_CAMS observation data, most regions of the world exhibit a decrease in occurrences of cold/dry extremes during 1985–2014 relative to 1955–1984, although there are some differences at the regional scale. Only in a few regions, such as parts of North and South America, parts of the Middle East, and parts of Asia, are there increases in cold/dry extremes. For compound cold/wet extremes, CRU and GHCN_CAMS observations show a decrease during 1985–2014 relative to 1955–1984, except for a few regions (such as parts of the southern United States, the west of Australia, and the Middle East) that show an increase. The locations where the occurrences of two compound cold extremes increase are very similar. Meanwhile, we found that the changes in compound extremes for cold/dry and cold/wet are similar, showing an overall decrease worldwide during 1985–2014 relative to 1955–1984. In the past few decades, the increases in occurrences of compound warm/dry and warm/wet extremes exceed the decreases for compound

cold/dry and cold/wet extremes, so the general trend is still toward warming (Deser et al., 2012; Hausfather et al., 2020; Wang et al., 2017).

Overall, most of the CMIP6 model simulations are basically consistent with the CRU and GHCN_CAMS observations (Figures 1 and S2–S5). However, there are still regional discrepancies in the performance across the models. Globally, the increase in the number of warm/dry extremes in tropical regions and high-latitudes is larger compared with other regions. The MME can simulate the spatial distribution of warm/dry extremes reasonably well, and the POD value is 0.78. Certain models, such as MPI-ESM1-2-HR and MIROC6, perform less well for warm/dry extremes, and both of the POD values are less than 0.65. For certain regions, especially the Amazon and North Africa, the simulation ability of the models for warm/dry extremes is relatively outstanding. For compound warm/wet extremes, the performance of most CMIP6 models is consistent with the observation results, and the POD values are around 0.7. But the number of increases in occurrences in the simulations still differs among the individual models. In addition, the simulations over Africa vary considerably by model. The difference in performance among models is large, probably because climate models represent a multitude of processes happening over various time and space scales, and they are simulated based on different assumptions about physical, chemical, and biological processes of the atmosphere, land, and oceans (Balaji et al., 2017; Papalexiou et al., 2020). The new generation of CMIP6 climate model has higher spatial resolution, new physical processes, and new biogeochemical cycles; these combinations lead to greater uncertainty among CMIP6 models (Jin et al., 2018). Moreover, studies have proven that CMIP6 models available have tended to show notably higher climate sensitivity than CMIP5 models, mainly due to cloud feedback (Voosen, 2019; Zelinka et al., 2020).

In general, the simulation performance for cold/dry extremes in most models is consistent with the observational results of CRU and GHCN_CAMS. The POD values of most models are less than 0.5. From a global perspective, the MME's simulation of the Southern Hemisphere is poor. However, for the simulations of some areas, there are large differences among the models. For example, most CMIP6 model simulations and observations show an increase for cold/dry extremes in the Amazon region, while a few models, such as CanESM5, CNRM-ESM2-1, EC-Earth3, and MPI-ESM1-2-HR, show a decrease. According to previous studies, the frequency of anomalous droughts over the Amazon region has increased due to increased greenhouse gas levels and continued human activity (Barkhordarian et al., 2019), and there have been serious fire disasters (Arruda et al., 2019). Looking specifically at China, another study has found that compound cold/dry extremes mainly occurred at high-latitudes and high altitudes across China (e.g., Northeast China and the Tibetan Plateau) (Liu et al., 2017). For cold/wet extremes, most CMIP6 models show reasonable consistency with observational data in most parts of the world, and they all show an overall decrease. The POD values of most models are around 0.6, and MIROC6 performs the worst, with a POD value of 0.49. For only a few regions, the models perform poorly in simulating CRU and GHCN_CAMS observations, and they even show an increase in some regions (e.g., the northern part of Eurasia). As with the warm/wet, warm/dry, and cold/dry compound extremes, there are still discrepancies between the models and the observations. For example, observations and simulations by most models show an increase in the eastern United States, while a few models indicate the opposite; previous research from CMIP5 showed similar discrepancies among the models in this region (Hao et al., 2013). Most CMIP5 models exhibit a decrease in the cold/wet extremes in eastern Australia (Hao et al., 2013), however, several CMIP6 models show the opposite result—notably, BBC-CSM2-MR, CESM2-WACCM, and MRI-ESM2-0.

With respect to the CRU observations, the POD values for warm/dry and warm/wet extremes are relatively high, while those for cold/dry and cold/wet extremes are relatively low. Among the models, CanESM5, CESM2, EC-Earth3-Veg, MRI-ESM2-0, and UKESM1-0-LL display higher consistency with the CRU observations. In addition, across all models, the ranges of variability in the POD values of the compound cold/dry and cold/wet extremes are greater than those of the warm/dry and warm/wet extremes, which is relatively consistent with previous findings (Hao et al., 2013). However, the POD values of the CMIP6 models for compound warm extremes are larger than those in CMIP5, suggesting that the performance of the compound warm extremes is somewhat improved in CMIP6. Meanwhile, compared with previous studies (Hao et al., 2013), we find that CMIP6's ability to characterize compound extremes for warm/dry and warm/wet is significantly improved relative to CMIP5. However, models cannot simulate the magnitudes of the compound extremes well. Furthermore, although the POD values can roughly show the skill of the CMIP6

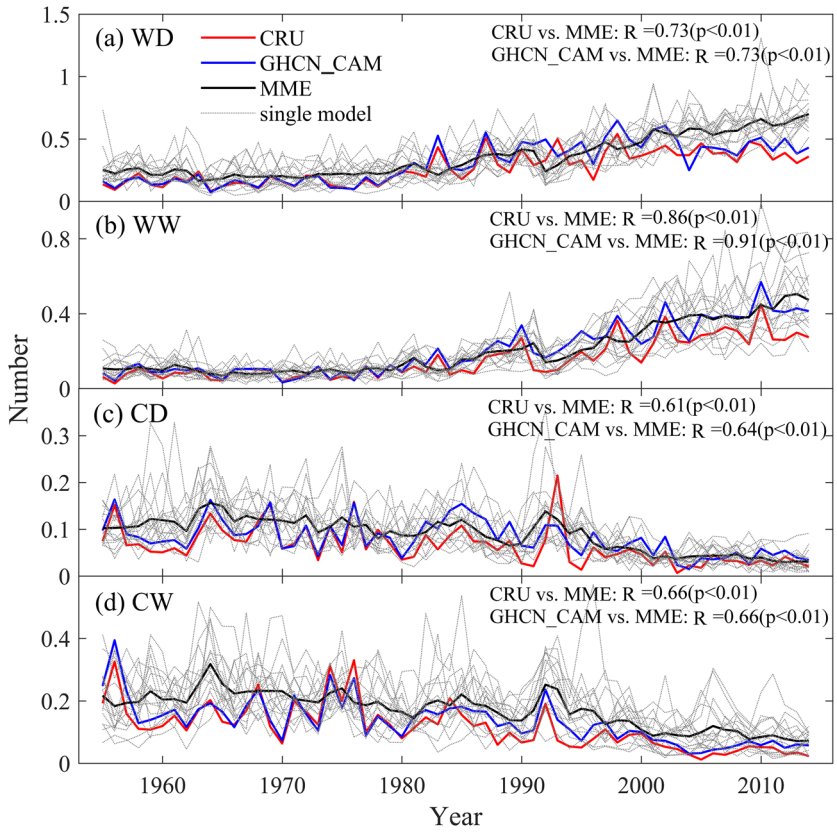

Figure 2. Temporal changes in the number of compound (a) warm/dry (WD), (b) warm/wet (WW), (c) cold/dry (CD), and (d) cold/wet (CW) extremes for the CRU and GHCN_CAMS observations, 16 CMIP6 models, and the MME during the period 1955–2014.

climate model products in detecting the occurrences of compound extremes for temperature and precipitation, another limitation is the fact that POD values evaluate only the total frequency of occurrence, without addressing whether the timing of simulated compound extremes is consistent with the timing of observed extremes (Dinku et al., 2010).

3.2. Temporal Changes

The temporal changes in the number of compound extremes from 1955 to 2014 show that there has been a significant increase in the frequency of compound warm/dry and warm/wet extremes but a decrease in the frequency of compound cold/dry and cold/wet extremes (Figure 2). Past studies have shown similar results for extreme events (Dashkhuu et al., 2015; Yan et al., 2002). The difference is that the occurrence of univariate extremes is stage-specific: the reduction in cool nights and cool days occurred over all four seasons, while the increase in warm days and warm nights occurred mainly in summer (Dashkhuu et al., 2015). Before 1985, the results from both the CRU and the GHCN_CAMS observations are almost the same, and after 1985, there is a notable difference. Meanwhile, we found that the increasing trends of compound warm/dry (0.56/100 yr (CRU) and 0.73/100 yr (GHCN_CAMS)) and warm/wet (0.47/100 yr (CRU) and 0.68/100 yr (GHCN_CAMS)) extremes are greater than the decreasing trends of compound cold/dry (0.11/100 yr (CRU) and 0.11/100 yr (GHCN_CAMS)) and cold/wet (0.28/100 yr (CRU) and 0.28/100 yr (GHCN_CAMS)) extremes over the world (Figure S6). From a regional perspective, the increasing trends of compound warm/dry and warm/wet extremes for CRU (GHCN_CAMS, in parentheses) over China are 1.80 (1.29) and 1.43 (1.37) times those over the world during the period 1955–2014. This shows that the increasing trend of warm/dry and warm/wet extremes over China is significantly higher than the global average level. Overall, the MME overestimates the temporal change in the numbers of the four types of extremes compared to the CRU and GHCN_CAMS observations, although it has better simulation performance than the individual

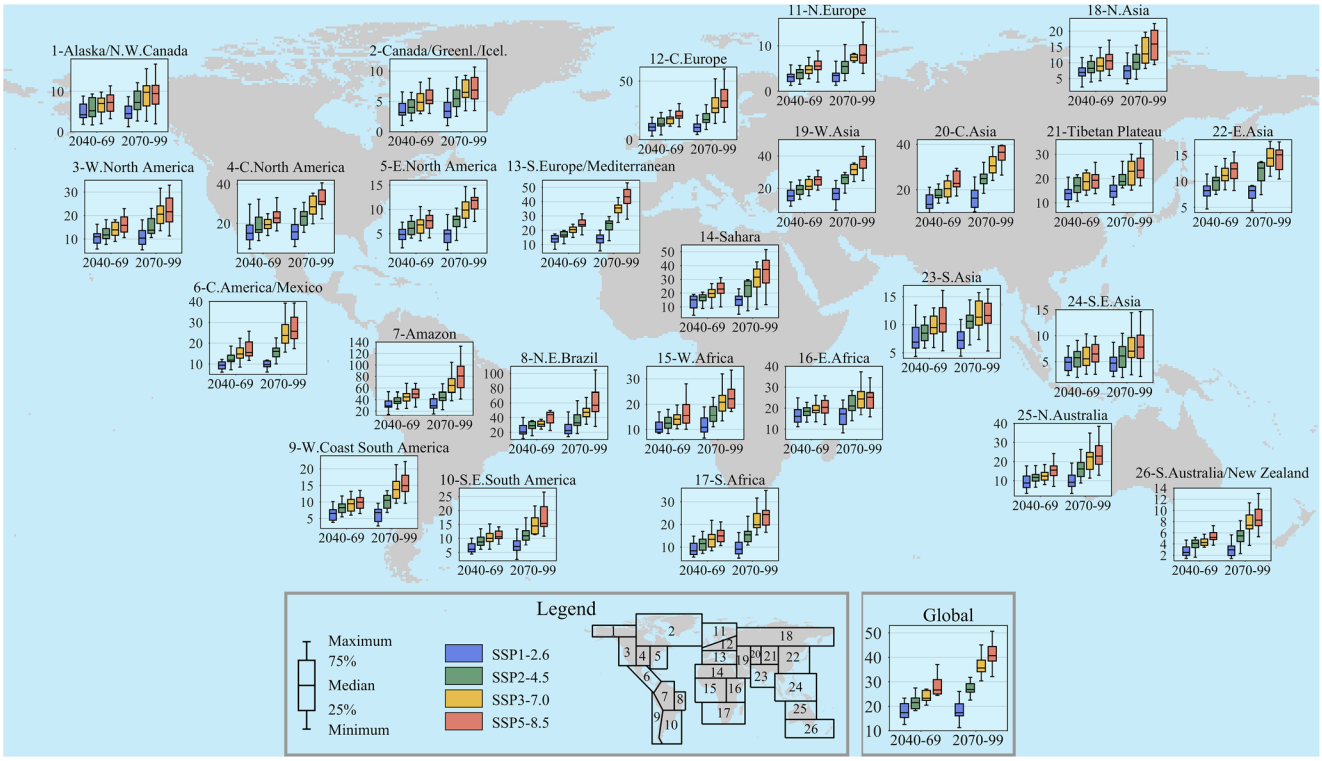

Figure 3. Future change in the frequency of occurrence of compound warm/dry extremes during two future periods, 2040–2069 and 2070–2099, relative to the period 1985–2014 under four different SSP scenarios (SSP1-2.6, SSP2-4.5, SSP3-7.0, and SSP5-8.5). The box plots show uncertainties among the models. See legend for defined extents of regions. The "Global" box displays the values computed using all land grid points (except Antarctica). To make up for the limitation of this spatial layout in which we show results for each global subregion, in Figure S9 we reproduce the subplots at larger scale.

models. Compared with the CRU observations, the temporal changes for MME in the number of compound extremes have higher correlation coefficients with the GHCN_CAMS observations, indicating better simulation performance. Out of the four types of compound extremes, the MME has the best simulation performance for warm/wet extremes, and the correlation coefficients are 0.86 (CRU) and 0.91 (GHCN_CAMS). Among the models, CanESM5, MRI-ESM2-0, UKESM1-0-LL, and the MME perform better in simulating the temporal changes in the numbers of the four compound extremes from 1955 to 2014. Especially for compound warm/wet extremes, the correlation coefficients approach up to about 0.8.

3.3. Future Changes and Uncertainty Analysis of Compound Extremes

According to the predictions of 16 models in CMIP6, the occurrences of both warm/dry and warm/wet extreme events will increase in the future; that is, under the four SSP scenarios, compound warm/dry and warm/wet extremes increase during the two future periods, 2040–2069 and 2070–2099, relative to the period 1985–2014 (Figures 3 and 4). Conversely, the occurrences of compound cold/dry and cold/wet extreme events will decrease in the future (Figures S7 and S8). This result is similar to findings from previous studies in CMIP5 (Wang et al., 2017), but in addition, we found that warm extremes tend to be more sensitive to global warming than cold ones. Furthermore, a large number of existing studies have also predicted that extreme events related to temperature (Pal & Eltahir, 2016) and precipitation (Donat et al., 2016; Prein et al., 2017) will continue to increase in the future. Among the regions we study, the Amazon (region 7), North-East Brazil (region 8), and the Tibetan Plateau (region 21) will have larger increases in compound warm/dry and warm/wet extremes than other regions worldwide; the associated consequences may include abnormal water temperatures in the Peru Current and a substantial reduction in production of fishery resources. Also, increased warm extreme events in southern Africa may lead to disease epidemics and discomfort or even death due to overheating. In general, under future scenarios, warm/wet extreme events increase faster than other modes of compound extremes under all of the SSPs (SSP1-2.6 to SSP5-8.5), and

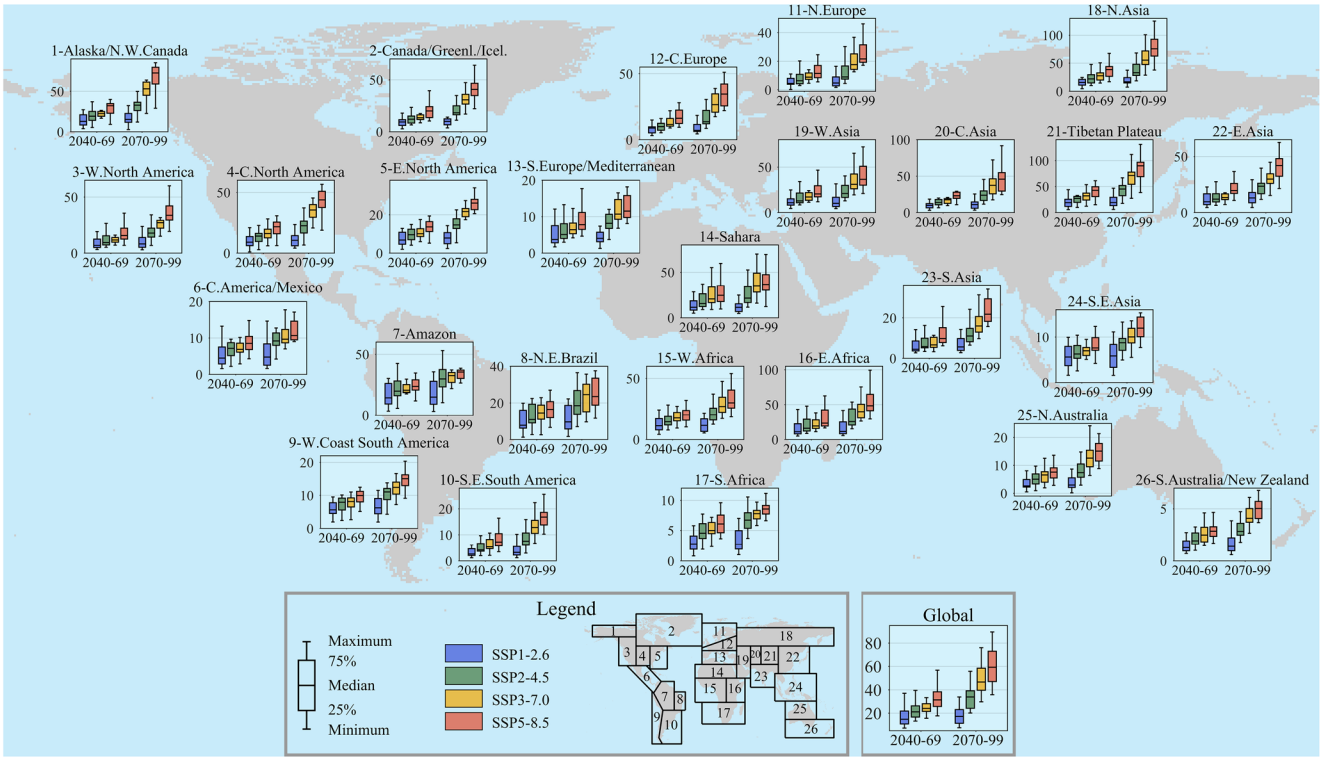

Figure 4. Same as Figure 3, but for compound warm/wet extremes. Corresponds to Figure S10.

each compound extreme in the long term (2070–2099) increases faster relative to the period 1985–2014 than the same type of extreme in the medium term (2040–2069). The Fifth Assessment Report of the IPCC also points out that the risks from climate change are larger in the long term than they are in the near term (IPCC, 2014). Warm/wet extremes are projected to exhibit larger changes relative to the period 1985–2014 under stronger versus weaker SSPs. Based on the changes in the global number of compound extremes, the average frequency of warm/wet extremes during the period 2040–2069 (and 2070–2099, in parentheses) is projected to increase relative to the period 1985–2014 by 17.18 (18.53), 22.69 (34.15), 26.58 (48.79), and 32.85 (59.60) under SSP1-2.6, SSP2-4.5, SSP3-7.0, and SSP5-8.5, respectively. Similar results also appeared in CMIP5 and manifested as RCP8.5 > RCP4.5 > RCP2.6 (Liu et al., 2017).

We also investigate the future change in the frequency of occurrence of compound extremes during two future periods, 2040–2069 and 2070–2099, relative to the period 1985–2014 under four SSP scenarios. The box plots show uncertainties among the models (Figures 3 and 4 and S7–S8). In these figures, the uncertainties among the models are indicated by the sizes of the colored boxes and the lengths of the whiskers. In our research, the distance between the 25th and 75th quantiles is used to represent the uncertainty range, based on previous studies (Yeh et al., 2009). The results show that the uncertainties among the models are relatively small for compound cold/dry and cold/wet extremes relative to the compound warm/dry and warm/wet extremes. Compared with the two types of compound cold extreme events, the two warm extremes of warm/dry and warm/wet have considerably higher uncertainties. The uncertainties in the numbers of the warm/wet extremes are the largest, and they are 2.01 and 3.82 times those of the warm/dry extremes in the medium term and long term, respectively. Recent research also shows that climate projections of future hot extremes exhibit large uncertainties regarding the magnitude of projected warming (Donat et al., 2018). For most regions, the uncertainties under the SSP5-8.5 scenario are larger than other scenarios. Therefore, we suspect that high-emission scenarios will bring greater uncertainty. From a regional perspective, South America and the Tibetan Plateau have greater uncertainties than other regions over the world. Several researchers have found that the climate change projections in the Amazon have a larger uncertainty range (Torres & Marengo, 2013), and we suspect that the Amazon may have contributed to the greater uncertainty of South America. As the Tibetan Plateau has the highest altitude in the world, it is easy to understand that

the uncertainty here is relatively large. For the warm/dry extremes, smaller uncertainties appear in several areas near the Arctic (e.g., Alaska/northwestern Canada (region 1), Canada/Greenland/Iceland (region 2), and northern Europe (region 11)). In addition, existing studies have quantified the causes of such uncertainties, including the internal variability, physical parameterizations, and so on (Solman & Pessacg, 2012). Certain studies also show that, regardless of the source of the uncertainties, the geographic distributions of the results across the ensemble members are consistent, especially for precipitation and temperature (Solman & Pessacg, 2012).

All four types of compound extreme events, it can be influenced by natural variability, including El Niño/Southern Oscillation, the North Atlantic Oscillation, the Pacific Decadal Oscillation, and so on (Geng et al., 2019; Grothe et al., 2020; Hamouda et al., 2021; Trenberth et al., 2014). The changes in the frequency of compound warm/dry extremes relate to the variation of precipitation and temperature associated with such patterns of variability. In the context of global warming, the increase in temperature may lead to more water being taken away by the evaporation part of the water cycle, thus causing some degree of drought (Dai, 2011; Vicente-Serrano et al., 2014). Due to the influence of land-atmosphere interactions, the arid climatic conditions can also cause an increase in temperature (Koster et al., 2016). Under global warming, heavy precipitation associated with tropical cyclones is projected to be higher at 2°C compared to 1.5°C of global warming (Hoegh-Guldberg et al., 2018). That is, the warming will bring more precipitation to equatorial and high-latitude regions (Feng et al., 2019). Further efforts are needed to understand the impact of global warming on the internal variability of the geophysical system, and then to fully understand how climate change drives the mechanisms that lead to compound events.

4. Conclusions and Prospective

In this study, we have investigated four types of compound temperature and precipitation extremes—warm/dry, warm/wet, cold/dry, and cold/wet—using ground-based observations and the recently released CMIP6 simulations. We found an overall increase in the global number of occurrences of warm/dry and warm/wet extremes during the period 1985–2014 relative to the period 1955–1984. Over the same time frame, the occurrences of cold/dry and cold/wet extremes decreased over most parts of world. We showed that most CMIP6 climate models can reproduce the four types of compound extremes mentioned above reasonably well compared with observations; however, some models exhibit discrepancies over certain areas. Overall, the models appear to perform poorly over low latitudes and tropical regions. POD values for compound warm/wet extremes are above 0.63, indicating good agreement in the sign of change between model simulations and ground-based observations for warm/wet extremes. The increasing trends of compound warm/dry and warm/wet extremes for CRU (GHCN_CAMS) over China are 1.80 (1.29) and 1.43 (1.37) times those worldwide during the period 1955–2014. Among the four types of compound extremes, the MME has the best simulation performance for temporal changes in warm/wet extremes, and correlation coefficients are 0.86 (CRU) and 0.91 (GHCN_CAMS).

Under the SSP scenarios, compound warm/dry and warm/wet extremes show a continuous increase in frequency in the next few decades, while compound cold/dry and cold/wet extremes are projected to occur less frequently. Globally, the average frequency of warm/wet extremes is projected to increase by 18.53, 34.15, 48.79, and 59.60 during the period 2070–2099 relative to the period 1985–2014 under SSP1-2.6, SSP2-4.5, SSP3-7.0, and SSP5-8.5, respectively. The uncertainties for compound warm/dry and warm/wet extremes increase considerably in the future; the uncertainties for warm/wet extremes are 2.01 (2040–2069) and 3.82 (2070–2099) times those of warm/dry extremes globally, and they are especially high for the Amazon and the Tibetan Plateau.

From the results relating to compound extremes in the future, we can speculate that the decreases in the numbers of compound cold/dry and cold/wet extremes may produce certain benefits for the natural environment and humans. For example, the reduction of cold damage and ice-snow disasters may be beneficial for the production of crops, and more importantly, it could reduce the casualties and economic losses caused by these disasters. On the other hand, changes in compound warm/dry and warm/wet extremes have a strong relationship with future precipitation under the continued warming projected for the future. Future precipitation changes are not only dependent on the temperature to a great extent but also related

to atmospheric circulation, storms, and other factors. So, the increases in compound warm/dry and warm/wet extremes will also have a number of profound negative effects on human health, agriculture, and infrastructure. In fact, warm/wet extremes are even more difficult to handle than warm/dry extremes, because humidity that is too high affects the human body's heat dissipation process. As the climate changes, abnormal temperatures and humidity will soon make parts of the Earth uninhabitable. Therefore, it is necessary for us to take effective measures to mitigate the adverse effects brought about by extreme heat. In sum, the results of this research can provide insights on climate model performance relevant to model developers, which will give us better tools to anticipate and address these issues. Also, the outcomes may be of interest to stakeholders working on reducing the risks associated with compound climate extremes.

Conflict of Interest

The authors declare that they have no conflict of interest.

Data Availability Statement

The CMIP6 model data sets that support the findings of this study are openly available at https://esgf-node.llnl.gov/projects/cmip6/. The observed climate data from the Climate Research Unit (CRU), Global Historical Climatology Network version 2 and the Climate Anomaly Monitoring System (GHCN + CAMS), and NOAA's Precipitation Reconstruction over Land (PREC/L) are available at https://crudata.uea.ac.uk/cru/data/hrg/cru_ts_4.03/, https://www.esrl.noaa.gov/psd/data/gridded/data.UDel_AirT_Precip.html, and http://www.psl.noaa.gov/data/gridded/data.precl.html.

Acknowledgments
This research was supported by the Second Tibetan Plateau Scientific Expedition and Research Program (STEP) (No. 2019QZKK0405) and the National Natural Science Foundation of China (No. 41877155).

References

Arruda, D., Candido, H. G., & Fonseca, R. (2019). Amazon fires threaten Brazil's agribusiness. *Science*, *365*(6460), 1387. https://doi.org/10.1126/science.aaz2198

Balaji, V., Maisonnave, E., Zadeh, N., Lawrence, B. N., Biercamp, J., Fladrich, U., et al. (2017). CPMIP: Measurements of real computational performance of Earth system models in CMIP6. *Geoscientific Model Development*, *10*(1), 19–34. https://doi.org/10.5194/gmd-10-19-2017

Barkhordarian, A., Saatchi, S. S., Behrangi, A., Loikith, P. C., & Mechoso, C. R. (2019). A recent systematic increase in vapor pressure deficit over Tropical South America. *Scientific Reports*, *9*(1), 15331. https://doi.org/10.1038/s41598-019-51857-8

Beniston, M., & Stephenson, D. B. (2004). Extreme climatic events and their evolution under changing climatic conditions. *Global and Planetary Change*, *44*(1), 1–9. https://doi.org/10.1016/j.gloplacha.2004.06.001

Casanueva, A., Herrera, S., Fernández, J., Frías, M. D., & Gutiérrez, J. M. (2013). Evaluation and projection of daily temperature percentiles from statistical and dynamical downscaling methods. *Natural Hazards and Earth System Sciences*, *13*(8), 2089–2099. https://doi.org/10.5194/nhess-13-2089-20110.5194/nhess-13-2089-2013

Chen, M., Xie, P., Janowiak, J. E., & Arkin, P. A. (2002). Global land precipitation: A 50 yr monthly analysis based on Gauge observations. *Journal of Hydrometeor*, *3*(3), 249–266. https://doi.org/10.1175/1525-7541(2002)003<0249:GLPAYM>2.0.CO;2

Ciavarella, A., Stott, P., & Lowe, J. (2017). Early benefits of mitigation in risk of regional climate extremes. *Nature Climate Change*, *7*(5), 326–330. https://doi.org/10.1038/nclimate3259

Dai, A. (2011). Drought under global warming: A review. *WIREs Climate Change*, *2*, 45–65. https://doi.org/10.1002/wcc.81

Dashkhuu, D., Kim, J. P., Chun, J. A., & Lee, W.-S. (2015). Long-term trends in daily temperature extremes over Mongolia. *Weather and Climate Extremes*, *8*, 26–33. https://doi.org/10.1016/j.wace.2014.11.003

Deser, C., Phillips, A., Bourdette, V., & Teng, H. (2012). Uncertainty in climate change projections: The role of internal variability. *Climate Dynamics*, *38*(3), 527–546. https://doi.org/10.1007/s00382-010-0977-x

Diaconescu, E. P., Gachon, P., & Laprise, R. (2015). On the remapping procedure of daily precipitation statistics and indices used in regional climate model evaluation. *Journal of Hydrometeorology*, *16*(6), 2301–2310. https://doi.org/10.1175/JHM-D-15-0025.1

Ding, T., Yuan, Y., Zhang, J., & Gao, H. (2019). 2018: The hottest summer in China and possible causes. *Journal of Meteorological Research*, *33*(4), 577–592. https://doi.org/10.1007/s13351-019-8178-y

Dinku, T., Ceccato, P., Cressman, K., & Connor, S. J. (2010). Evaluating detection skills of satellite rainfall estimates over desert Locust Recession regions. *Journal of Applied Meteorology and Climatology*, *49*(6), 1322–1332. https://doi.org/10.1175/2010JAMC2281.1

Donat, M. G., Lowry, A. L., Alexander, L. V., O'Gorman, P. A., & Maher, N. (2016). More extreme precipitation in the world's dry and wet regions. *Nature Climate Change*, *6*(5), 508–513. https://doi.org/10.1038/nclimate2941

Donat, M. G., Pitman, A. J., & Angélil, O. (2018). Understanding and reducing future uncertainty in midlatitude daily heat extremes via land surface feedback constraints. *Geophysical Research Letters*, *45*(19), 10627–10636. https://doi.org/10.1029/2018GL079128

Eggen, M., Ozdogan, M., Zaitchik, B., Ademe, D., Foltz, J., & Simane, B. (2019). Vulnerability of sorghum production to extreme, sub-seasonal weather under climate change. *Environmental Research Letters*, *14*(4), 045005. https://doi.org/10.1088/1748-9326/aafe19

Estrella, N., & Menzel, A. (2013). Recent and future climate extremes arising from changes to the bivariate distribution of temperature and precipitation in Bavaria, Germany. *International Journal of Climatology*, *33*(7), 1687–1695. https://doi.org/10.1002/joc.3542

Eyring, V., Cox, P. M., Flato, G. M., Gleckler, P. J., Abramowitz, G., Caldwell, P., et al. (2019). Taking climate model evaluation to the next level. *Nature Climate Change*, *9*(2), 102–110. https://doi.org/10.1038/s41558-018-0355-y

Fan, Y., & van den Dool, H. (2008). A global monthly land surface air temperature analysis for 1948-present. *Journal of Geophysical Research*, *113*(D1). https://doi.org/10.1029/2007JD008470

Feng, X., Liu, C., Xie, F., Lu, J., Chiu, L. S., Tintera, G., & Chen, B. (2019). Precipitation characteristic changes due to global warming in a high-resolution (16 km) ECMWF simulation. *Quarterly Journal of the Royal Meteorological Society*, *145*(718), 303–317. https://doi.org/10.1002/qj.3432

Fink, A. H., Brücher, T., Krüger, A., Leckebusch, G. C., Pinto, J. G., & Ulbrich, U. (2004). The 2003 European summer heatwaves and drought-synoptic diagnosis and impacts. *Weather*, *59*(8), 209–216. https://doi.org/10.1256/wea.73.04

Fischer, E. M., & Knutti, R. (2015). Anthropogenic contribution to global occurrence of heavy-precipitation and high-temperature extremes. *Nature Climate Change*, *5*(6), 560–564. https://doi.org/10.1038/nclimate2617

Geng, T., Yang, Y., & Wu, L. (2019). On the mechanisms of Pacific Decadal oscillation modulation in a warming climate. *Journal of Climate*, *32*(5), 1443–1459. https://doi.org/10.1175/jcli-d-18-0337.1

Gidden, M. J., Riahi, K., Smith, S. J., Fujimori, S., Luderer, G., Kriegler, E., et al. (2019). Global emissions pathways under different socioeconomic scenarios for use in CMIP6: A data set of harmonized emissions trajectories through the end of the century. *Geoscientific Model Development*, *12*(4), 1443–1475. https://doi.org/10.5194/gmd-12-1443-2019

Gou, J., Miao, C., Samaniego, L., Xiao, M., Wu, J., & Guo, X. (2021). CNRD v1.0: A high-quality natural runoff data set for hydrological and climate studies in China. *Bulletin of the American Meteorological Society*, 1–57. https://doi.org/10.1175/BAMS-D-20-0094.1

Grothe, P. R., Cobb, K. M., Liguori, G., Di Lorenzo, E., Capotondi, A., Lu, Y., et al. (2020). Enhanced El Niño-Southern oscillation variability in recent decades. *Geophysical Research Letters*, *47*(7), e2019GL083906. https://doi.org/10.1029/2019GL083906

Gusain, A., Ghosh, S., & Karmakar, S. (2020). Added value of CMIP6 over CMIP5 models in simulating Indian summer monsoon rainfall. *Atmospheric Research*, *232*, 104680. https://doi.org/10.1016/j.atmosres.2019.104680

Hamouda, M. E., Pasquero, C., & Tziperman, E. (2021). Decoupling of the Arctic oscillation and North Atlantic oscillation in a warmer climate. *Nature Climate Change*, *11*, 137–142. https://doi.org/10.1038/s41558-020-00966-8

Hao, Z., AghaKouchak, A., & Phillips, T. J. (2013). Changes in concurrent monthly precipitation and temperature extremes. *Environmental Research Letters*, *8*(3), 034014. https://doi.org/10.1088/1748-9326/8/3/034014

Hao, Z., Phillips, T. J., Hao, F., & Wu, X. (2019). Changes in the dependence between global precipitation and temperature from observations and model simulations. *International Journal of Climatology*, *39*(12), 4895–4906. https://doi.org/10.1002/joc.6111

Harris, I., Jones, P. D., Osborn, T. J., & Lister, D. H. (2014). Updated high-resolution grids of monthly climatic observations - the CRU TS3.10 Data set. *International Journal of Climatology*, *34*(3), 623–642. https://doi.org/10.1002/joc.3711

Hausfather, Z., Drake, H. F., Abbott, T., & Schmidt, G. A. (2020). Evaluating the performance of past climate model projections. *Geophysical Research Letters*, *47*(1), e2019GL085378. https://doi.org/10.1029/2019GL085378

Hoegh-Guldberg, O., Jacob, D., Taylor, M., Bindi, M., Brown, S., Camilloni, I., et al. (2018). Impacts of 1.5ºC global warming on natural and human systems. In V. Masson-Delmotte, P. Zhai, H.-O. Pörtner, D. Roberts, J. Skea, P. R. Shukla, et al. (Eds.), *Global Warming of 1.5°C. An IPCC Special Report on the impacts of global warming of 1.5°C above pre-industrial levels and related global greenhouse gas emission pathways, in the context of strengthening the global response to the threat of climate change, sustainable development, and efforts to eradicate poverty*.

IPCC. (2014). Summary for policymakers. In C. B. Field, V. R. Barros, D. J. Dokken, K. J. Mach, M. D. Mastrandrea, T. E. Bilir, et al. (Eds.), *Climate change 2014: Impacts, adaptation, and vulnerability. Part A: Global and sectoral aspects. Contribution of Working Group II to the Fifth Assessment Report of the Intergovernmental Panel on Climate Change* (pp. 1–32). Cambridge University Press.

Jin, M., Deal, C., Maslowski, W., Matrai, P., Roberts, A., Osinski, R., et al. (2018). Effects of model resolution and ocean mixing on forced Ice-Ocean physical and biogeochemical simulations using global and regional system models. *Journal of Geophysical Research: Oceans*, *123*, 358–377. https://doi.org/10.1002/2017jc013365

Kim, Y.-H., Min, S.-K., Zhang, X., Sillmann, J., & Sandstad, M. (2020). Evaluation of the CMIP6 multi-model ensemble for climate extreme indices. *Weather and Climate Extremes*, *29*, 100269. https://doi.org/10.1016/j.wace.2020.100269

Koster, R. D., Chang, Y., Wang, H., & Schubert, S. D. (2016). Impacts of local soil moisture anomalies on the atmospheric circulation and on remote surface meteorological fields during boreal summer: A comprehensive analysis over North America. *Journal of Climate*, *29*(20), 7345–7364. https://doi.org/10.1175/jcli-d-16-0192.1

Leonard, M., Westra, S., Phatak, A., Lambert, M., van den Hurk, B., McInnes, K., et al. (2014). A compound event framework for understanding extreme impacts. *WIREs Climate Change*, *5*(1), 113–128. https://doi.org/10.1002/wcc.252

Li, X., You, Q., Ren, G., Wang, S., Zhang, Y., Yang, J., & Zheng, G. (2019). Concurrent droughts and hot extremes in northwest China from 1961 to 2017. *International Journal of Climatology*, *39*(4), 2186–2196. https://doi.org/10.1002/joc.5944

Liu, F., Zhao, T., Wang, B., Liu, J., & Luo, W. (2018). Different global precipitation responses to solar, volcanic, and greenhouse gas forcings. *Journal of Geophysical Research: Atmospheres*, *123*(8), 4060–4072. https://doi.org/10.1029/2017JD027391

Liu, J., Du, H., Wu, Z., He, H. S., Wang, L., & Zong, S. (2017). Recent and future changes in the combination of annual temperature and precipitation throughout China. *International Journal of Climatology*, *37*(2), 821–833. https://doi.org/10.1002/joc.4742

Miao, C., Duan, Q., Sun, Q., Huang, Y., Kong, D., Yang, T., et al. (2014). Assessment of CMIP5 climate models and projected temperature changes over Northern Eurasia. *Environmental Research Letters*, *9*(5), 055007. https://doi.org/10.1088/1748-9326/9/5/055007

Miao, C., Sun, Q., Duan, Q., & Wang, Y. (2016). Joint analysis of changes in temperature and precipitation on the Loess Plateau during the period 1961–2011. *Climate Dynamics*, *47*(9), 3221–3234. https://doi.org/10.1007/s00382-016-3022-x

Nie, S., Fu, S., Cao, W., & Jia, X. (2020). Comparison of monthly air and land surface temperature extremes simulated using CMIP5 and CMIP6 versions of the Beijing climate center climate model. *Theoretical and Applied Climatology*, *140*(1), 487–502. https://doi.org/10.1007/s00704-020-03090-x

O'Neill, B. C., Tebaldi, C., van Vuuren, D. P., Eyring, V., Friedlingstein, P., Hurtt, G., et al. (2016). The Scenario Model Intercomparison Project (ScenarioMIP) for CMIP6. *Geoscientific Model Development*, *9*(9), 3461–3482. https://doi.org/10.5194/gmd-9-3461-2016

Oliver, E. C. J., Donat, M. G., Burrows, M. T., Moore, P. J., Smale, D. A., Alexander, L. V., et al. (2018). Longer and more frequent marine heatwaves over the past century. *Nature Communications*, *9*(1), 1324. https://doi.org/10.1038/s41467-018-03732-9

Pal, J. S., & Eltahir, E. A. B. (2016). Future temperature in southwest Asia projected to exceed a threshold for human adaptability. *Nature Climate Change*, *6*(2), 197–200. https://doi.org/10.1038/nclimate2833

Papalexiou, S. M., & Montanari, A. (2019). Global and regional increase of precipitation extremes under global warming. *Water Resources Research*, *55*(6), 4901–4914. https://doi.org/10.1029/2018WR024067

Papalexiou, S. M., Rajulapati, C. R., Clark, M. P., & Lehner, F. (2020). Robustness of CMIP6 historical global mean temperature simulations: Trends, long-term persistence, autocorrelation, and distributional shape. *Earth's Future*, *8*, e2020EF001667. https://doi.org/10.1029/2020EF001667

Prein, A. F., Rasmussen, R. M., Ikeda, K., Liu, C., Clark, M. P., & Holland, G. J. (2017). The future intensification of hourly precipitation extremes. *Nature Climate Change*, *7*(1), 48–52. https://doi.org/10.1038/nclimate3168

Rahmstorf, S., & Coumou, D. (2011). Increase of extreme events in a warming world. *Proceedings of the National Academy of Sciences*, *108*(44), 17905–17909. https://doi.org/10.1073/pnas.1101766108
Raymond, C., Matthews, T., & Horton, R. M. (2020). The emergence of heat and humidity too severe for human tolerance. *Science Advances*, *6*(19), eaaw1838. https://doi.org/10.1126/sciadv.aaw1838
Riahi, K., van Vuuren, D. P., Kriegler, E., Edmonds, J., O'Neill, B. C., Fujimori, S., et al. (2017). The shared socioeconomic pathways and their energy, land use, and greenhouse gas emissions implications: An overview. *Global Environmental Change*, *42*, 153–168. https://doi.org/10.1016/j.gloenvcha.2016.05.009
Sadegh, M., Moftakhari, H., Gupta, H. V., Ragno, E., Mazdiyasni, O., Sanders, B., et al. (2018). Multihazard scenarios for analysis of compound extreme events. *Geophysical Research Letters*, *45*(11), 5470–5480. https://doi.org/10.1029/2018GL077317
Semmler, T., Danilov, S., Gierz, P., Goessling, H. F., Hegewald, J., Hinrichs, C., et al. (2020). Simulations for CMIP6 With the AWI climate model AWI-CM-1-1. *Journal of Advances in Modeling Earth Systems*, *12*, e2019MS002009. https://doi.org/10.1029/2019MS002009
Seneviratne, S. I., Nichols, N., Easterling, D., Goodess, C. M., Kanae, S., Kossin, J., et al. (2012). Changes in climate extremes and their impacts on the natural physical environment. In C. B. Field, V. Barros, T. F. Stocker, D. Qin, D. J. Dokken, K. L. Ebi, et al. (Eds.), *Managing the risks of extreme events and disasters to advance climate change adaptation*. [A Special Report of Working Groups I and II of the Intergovernmental Panel on Climate Change (IPCC)] (pp. 109–230). Cambridge University Press.
Sharma, S., & Mujumdar, P. (2017). Increasing frequency and spatial extent of concurrent meteorological droughts and heatwaves in India. *Scientific Reports*, *7*(1), 15582. https://doi.org/10.1038/s41598-017-15896-3
Solman, S. A., & Pessacg, N. L. (2012). Evaluating uncertainties in regional climate simulations over South America at the seasonal scale. *Climate Dynamics*, *39*(1), 59–76. https://doi.org/10.1007/s00382-011-1219-6
Sun, Q., Miao, C., Hanel, M., Borthwick, A. G. L., Duan, Q., Ji, D., & Li, H. (2019). Global heat stress on health, wildfires, and agricultural crops under different levels of climate warming. *Environment International*, *128*, 125–136. https://doi.org/10.1016/j.envint.2019.04.025
Sun, Y., Zhang, X., Zwiers, F. W., Song, L., Wan, H., Hu, T., et al. (2014). Rapid increase in the risk of extreme summer heat in Eastern China. *Nature Climate Change*, *4*(12), 1082–1085. https://doi.org/10.1038/nclimate2410
Tian, B., & Dong, X. (2020). The double-ITCZ bias in CMIP3, CMIP5, and CMIP6 models based on annual mean precipitation. *Geophysical Research Letters*, *47*(8), e2020GL087232. https://doi.org/10.1029/2020GL087232
Torres, R. R., & Marengo, J. A. (2013). Uncertainty assessments of climate change projections over South America. *Theoretical and Applied Climatology*, *112*(1), 253–272. https://doi.org/10.1007/s00704-012-0718-7
Trenberth, K. E., Dai, A., van der Schrier, G., Jones, P. D., Barichivich, J., Briffa, K. R., & Sheffield, J. (2014). Global warming and changes in drought. *Nature Climate Change*, *4*(1), 17–22. https://doi.org/10.1038/nclimate2067
Trenberth, K. E., & Fasullo, J. T. (2012). Climate extremes and climate change: The Russian heat wave and other climate extremes of 2010. *Journal of Geophysical Research: Atmospheres*, *117*(D17), D17103. https://doi.org/10.1029/2012JD018020
Vicente-Serrano, S. M., Lopez-Moreno, J.-I., Beguería, S., Lorenzo-Lacruz, J., Sanchez-Lorenzo, A., García-Ruiz, J. M., et al. (2014). Evidence of increasing drought severity caused by temperature rise in southern Europe. *Environmental Research Letters*, *9*(4), 044001. https://doi.org/10.1088/1748-9326/9/4/044001
Vincent, L. A., Zhang, X., Mekis, É., Wan, H., & Bush, E. J. (2018). Changes in Canada's climate: Trends in indices based on daily temperature and precipitation data. *Atmosphere-Ocean*, *56*, 332–349. https://doi.org/10.1080/07055900.2018.1514579
Voosen, P. (2019). New climate models forecast a warming surge. *Science*, *364*(6437), 222. https://doi.org/10.1126/science.364.6437.222
Wang, X., Jiang, D., & Lang, X. (2017). Future extreme climate changes linked to global warming intensity. *Science Bulletin*, *62*(24), 1673–1680. https://doi.org/10.1016/j.scib.2017.11.004
Wang, Y., Ding, Z., & Ma, Y. (2019). Spatial and temporal analysis of changes in temperature extremes in the non-monsoon region of China from 1961 to 2016. *Theoretical and Applied Climatology*, *137*(3), 2697–2713. https://doi.org/10.1007/s00704-019-02767-2
Wasko, C., & Sharma, A. (2017). Global assessment of flood and storm extremes with increased temperatures. *Scientific Reports*, *7*(1), 7945. https://doi.org/10.1038/s41598-017-08481-1
Wu, X., Hao, Z., Zhang, X., Li, C., & Hao, F. (2020). Evaluation of severity changes of compound dry and hot events in China based on a multivariate multi-index approach. *Journal of Hydrology*, *583*, 124580. https://doi.org/10.1016/j.jhydrol.2020.124580
Wu, Y., Miao, C., Duan, Q., Shen, C., & Fan, X. (2020). Evaluation and projection of daily maximum and minimum temperatures over China using the high-resolution NEX-GDDP dataset. *Climate Dynamics*, *55*(9), 2615–2629. https://doi.org/10.1007/s00382-020-05404-1
Yan, Z., Jones, P. D., Davies, T. D., Moberg, A., Bergström, H., Camuffo, D., et al. (2002). Trends of extreme temperatures in Europe and China based on daily observations. *Climatic Change*, *53*(1), 355–392. https://doi.org/10.1023/A:1014939413284
Yang, Z., Wang, Q., & Liu, P. (2019). Extreme temperature and mortality: Evidence from China. *International Journal of Biometeorology*, *63*(1), 29–50. https://doi.org/10.1007/s00484-018-1635-y
Yeh, C. C., Wang, K. M., & Suen, Y. B. (2009). Quantile analyzing the dynamic linkage between inflation uncertainty and inflation. *Problems and Perspectives in Management*, *7*, 21–28.
You, Q., Jiang, Z., Wang, D., Pepin, N., & Kang, S. (2018). Simulation of temperature extremes in the Tibetan Plateau from CMIP5 models and comparison with gridded observations. *Climate Dynamics*, *51*(1), 355–369. https://doi.org/10.1007/s00382-017-3928-y
Zelinka, M. D., Myers, T. A., McCoy, D. T., Po-Chedley, S., Caldwell, P. M., Ceppi, P., et al. (2020). Causes of higher climate sensitivity in CMIP6 models. *Geophysical Research Letters*, *47*, e2019GL085782. https://doi.org/10.1029/2019GL085782
Zhang, W., & Villarini, G. (2017). Heavy precipitation is highly sensitive to the magnitude of future warming. *Climatic Change*, *145*(1), 249–257. https://doi.org/10.1007/s10584-017-2079-9
Zhou, B., Xu, Y., Wu, J., Dong, S., & Shi, Y. (2016). Changes in temperature and precipitation extreme indices over China: Analysis of a high-resolution grid data set. *International Journal of Climatology*, *36*(3), 1051–1066. https://doi.org/10.1002/joc.4400
Zhou, P., & Liu, Z. (2018). Likelihood of concurrent climate extremes and variations over China. *Environmental Research Letters*, *13*(9), 094023. https://doi.org/10.1088/1748-9326/aade9e
Zhou, T., & Chen, X. (2015). Uncertainty in the 2°C warming threshold related to climate sensitivity and climate feedback. *Journal of Meteorological Research*, *29*(6), 884–895. https://doi.org/10.1007/s13351-015-5036-4
Zscheischler, J., & Seneviratne, S. I. (2017). Dependence of drivers affects risks associated with compound events. *Science Advances*, *3*(6), e1700263. https://doi.org/10.1126/sciadv.1700263